Responses to Referee #1's comments

We are grateful to the reviewers for their valuable and helpful comments on our manuscript "Rapid formation of hydroxymethyl hydroperoxide and its vital role in methanesulfonic acid-methylamine nucleation: impacts of urban industrial and forested areas" (MS No.: **egusphere-2025-4960**). We have revised the manuscript carefully according to reviewers' comments. The point-to-point responses to the Referee #1's comments are summarized below:

General comments:

Publisher's note: this comment was edited on 1 December 2025. The following text is not identical to the original comment, but the adjustments were minor without effect on the scientific meaning.

The manuscript by Li et al. presents a detailed theoretical investigation into the formation mechanism of hydroxymethyl hydroperoxide (HMHP) via methanesulfonic acid (MSA)-catalyzed hydrolysis of CH_2OO in both the gas phase and at the air-water interface, and its significant role in enhancing MSA-methylamine (MA)-driven new particle formation (NPF). This study employed quantum chemical calculations, Born-Oppenheimer molecular dynamics simulations, and atmospheric cluster dynamics code to provide molecular-level insights into the catalytic effect of MSA and the promoting role of HMHP in nucleation. This study enhances our understanding of HMHP in the atmosphere. I recommend publication of this manuscript after consideration of the following comments:

Specific Comments:

Comment 1.

In the Introduction, the linkage between the first and second paragraphs could be strengthened.

Response: Thanks for your valuable comments. In response to the reviewer's suggestion, we have added a sentence in Lines 42-44 on Page 2 of the revised manuscript to improve the logical transition between the first and second paragraphs. Specifically, the added sentence states that "HMHP is formed predominantly through the hydrolysis of CH_2OO, a process that has been extensively investigated through both experimental studies (Chao et al., 2015; Stone et al., 2014; Berndt et al., 2015) and theoretical simulations (Wu et al., 2023a; Lin et al., 2016; Wu et al., 2023b)".

Comment 2.

The computational details for BOMD calculation and ACDC simulations, such as the set of wall, the definition of boundary clusters, the values of coagulation sinks, and so on, should be more thoroughly described in the main text or supplementary information to ensure reproducibility.

Response: Thanks for your valuable comments. As the reviewer's suggestion, the details of the BOMD calculations and ACDC simulations have been substantially expanded in the manuscript and supplement. The corresponding main revision has been made as follows.

(a) Regarding the issue of the "set of wall" in BOMD simulations, the BOMD simulations conducted in this study did not employ such "wall" constraints or potential functions. All simulations were performed under standard periodic boundary conditions, without introducing additional spatial restrictions or boundary potentials. To ensure the reproducibility of this study, the complete BOMD computational parameters and setup details have been presented in the Part S3 of the supplement. This section comprehensively lists all key parameters, including the software used, functional, basis set, integration step size, temperature control scheme, total simulation duration, and the handling of periodic boundary conditions.

(b) Within the ACDC simulations, external losses were estimated using a fixed condensation sink coefficient of 2.6 × 10^{-3} s^{-1}. In Lines 157-158 on Page 6 of the revised manuscript, the sentence of "External losses of cluster *i* were represented using a fixed condensation sink coefficient of 0.02 s^{-1} (Qiao et al., 2024; Zhang et al., 2022)." has been added.

(c) Within the ACDC simulations, boundary clusters are those allowed to flux out of the simulation box for further growth. Consequently, the smallest clusters outside the simulated system must be sufficiently stable to prevent immediate evaporation back into the system. Based on Gibbs free energies (Table S7) and total evaporation rates (Table S9), $(MSA)_4{\cdot}(MA)_3$ and $(MSA)_4{\cdot}(MA)_4$ were selected as boundary clusters due to their lower Gibbs free energy and evaporation rates compared to the binary MSA-MA and HMHP-inclusive clusters. So, in Lines 159-160 on Page 6 of the revised manuscript, the sentence of "Besides, the clusters $(MSA)_4{\cdot}(MA)_3$ and $(MSA)_4{\cdot}(MA)_4$ were selected as boundary clusters in the MSA-MA-HMHP system, as boundary clusters in ACDC are required to be sufficiently stable to allow continued growth.." has been added.

(d) Within the ACDC simulations, the calculation methods for $\beta_{i,j}$ and $\gamma_{(i+j)\rightarrow i}$ are shown in the Part S5 of the supplement.

Comment 3.

Lines 143, why was the energy at the DLPNO-CCSD(T)-F12/cc-pVDZ-F12-CABS level not used as the thermodynamic data input for ACDC?

Response: Thanks for your valuable comments. We sincerely apologize for using an incorrect and misleading expression in the description of the thermodynamic data used as input for ACDC. Indeed, in this work, the Gibbs free energy changes (Δ*G*) of the clusters, calculated at the DLPNO-CCSD(T)-F12/cc-pVDZ-F12-CABS//M06-2X/6-311++G(2df,2pd) level of theory, were incorporated as input files for the ACDC simulations. So, in Lines 149-151 on Page 6 of the revised manuscript, the sentence of "Thermodynamic data, calculated at the M06-2X/6-311++G(2df,2pd) level of theory, were employed as input parameters for the ACDC simulations." has been changed as "Thermodynamic data, calculated at the DLPNO-CCSD(T)-F12/cc-pVDZ-F12-CABS//M06-2X/6-311++G(2df,2pd) level of theory, were employed as input parameters for the ACDC simulations."

Comment 4.

The Methods section should state the version of ORCA employed.

Response: Thanks for your valuable comments. As the reviewer's suggestion, we have revised Section 2.1 (Quantum Chemical Calculations) to explicitly specify the software version used. All quantum chemical calculations in this work were performed with the ORCA 4.2.0 package. So, in Lines 109 on Page 4 of the revised manuscript, the sentence of "Subsequently, the ORCA 4.2.0 package (Neese, 2012) was performed to compute the single point energies using the CCSD(T)-F12/cc-pVDZ-F12 method." has been added.

Comment 5.

Lines 160-162, how were the concentrations of MSA···H_2O and CH_2OO···H_2O calculated?

Response: Thanks for your valuable comments. The steady-state concentrations of MSA···H_2O and CH_2OO···H_2O were calculated using the corresponding calculated equilibrium constant (***Nat.***

Commun., 2023, 14, 498; ***Phys. Chem. Chem. Phys.***, 2023, 25, 28205-28212; ***J. Phys. Chem. A*****,** 2019, 123, 8448-8459). Based on this, the main revisions have been made as described below.

(a) In Line 171 on Page 6 of the revised manuscript, we have added the sources of the concentrations for $MSA\cdots H_2O$ and $CH_2OO\cdots H_2O$. Specifically, the following statement has been included: "Considering the atmosphere concentrations of MSA (Li et al., 2024b), H_2O (Anglada et al., 2013), and CH_2OO (Khan et al., 2018), the concentration of $MSA\cdots H_2O$ is two orders of magnitude greater than that of $CH_2OO\cdots H_2O$, as shown in Table S3, predicting that the $MSA\cdots H_2O$ + CH_2OO route is the dominant pathway for the MSA-catalyzed reaction".

(b) The computational details for deriving the concentrations of $MSA\cdots H_2O$ and $CH_2OO\cdots H_2O$ are presented below Table S3 in the supplement.

Atmospheric concentrations of $MSA\cdots H_2O$ and $CH_2OO\cdots H_2O$ within the temperature range of 280.0-320.0 K

The steady-state concentration of $MSA\cdots H_2O$ and $CH_2OO\cdots H_2O$ were calculated using the calculated equilibrium constant listed in Eq. S1 and Eq. S2, respectively.

$$K_{eq1} = \frac{[MSA\cdots H_2O]}{[H_2O][MSA]} \tag{S1}$$

$$K_{eq2} = \frac{[CH_2OO\cdots H_2O]}{[H_2O][CH_2OO]} \tag{S2}$$

where K_{eq1} and K_{eq2} are the equilibrium constants ($cm^3\cdot molecule^{-1}$) for the complexes of $MSA\cdots H_2O$ and $CH_2OO\cdots H_2O$ within the temperature range of 280.0-320.0 K shown in Table S2, respectively. Atmospheric concentrations of MSA, H_2O and CH_2OO were taken from references (*J. Am. Chem. Soc.* **2018,** *140*, 35, 11020-11028).

Comment 6.

Lines 172-183, what is the conclusion of this section? Based on these effective rate constants, is H_2O the most effective catalyst?

Response: Thanks for your valuable comments. Based on the calculated effective rate constants, MSA exhibits significantly higher catalytic activity than NH_3 and SA. Nevertheless, its catalytic efficiency remains lower than that of H_2O. In Lines 185-193 on Page 7 of the revised manuscript, the sentence of "When the MSA concentration ranges from 10^6 to 10^8 molecules·cm^{-3}, its catalytic effect is substantially stronger than that of NH_3 ([NH_3] = 10^7-10^{11} molecules·cm^{-3}), with k'_{MSA} being approximately 2-6 orders of magnitude over the temperature range of 280.0-320.0 K. Similarly, for MSA concentrations between 10^5 and 10^8 molecules·cm^{-3}, MSA exhibits a significantly higher catalytic activity than SA ([SA] = 10^4-10^7 molecules·cm^{-3}). In this case, k'_{MSA} exceeds k'_{SA} by about 1-3 orders of magnitude. Taken together, these results demonstrate that MSA is a more effective catalyst than both NH_3 and SA under atmospherically relevant conditions. Nevertheless, even under extreme conditions, with MSA at its upper-limit concentration ([MSA] = 10^8 molecules·cm^{-3}) and H_2O at its lower-limit concentration ([H_2O] = 10^{16} molecules·cm^{-3}), k'_{MSA} is approximately five orders of magnitude smaller than $k'_{WM,,}$ indicating that the catalytic efficiency of MSA remains lower than that of H_2O." has been reorganized.

Comment 7.

In Section 3.3.2, the discussion on evaporation rates and stability is rather limited and unclear. Moreover, it closely resembles the descriptions provided in the pathway section.

Response: Thanks for your valuable comments. We apologize that the description of cluster thermodynamic stability in Section 3.3.2 was not sufficiently clear. As the reviewer's suggestion, based on the Gibbs free energy (ΔG) (Table S7) and total evaporation rates ($\Sigma\gamma$) (Table S10) of clusters, we have replaced the ΔG in Fig. 4 with the collision-to-evaporation ratio ($\beta C/\Sigma\gamma$) and reorganized Section 3.3.2 accordingly. The detailed revisions are outlined below.

(a) Based on the ΔG (Table S7) and $\Sigma\gamma$ (Table S10) of the clusters, the $\beta C/\Sigma\gamma$ were calculated. The $\beta C/\Sigma\gamma$ quantifies the competition between cluster growth and evaporative dissipation, serving as a key kinetic indicator for determining whether clusters can stably exist and grow in the atmosphere (***Environ. Sci. Technol.***, 2025, 59, 22772-22783; ***Sci. Total Environ.***, 2023, 859, 159832; ***Environ. Res. Lett.***, 2024, 19, 014076). Therefore, the revised Fig. 4 has been reorganized to present the $\beta C/\Sigma\gamma$ ratio.

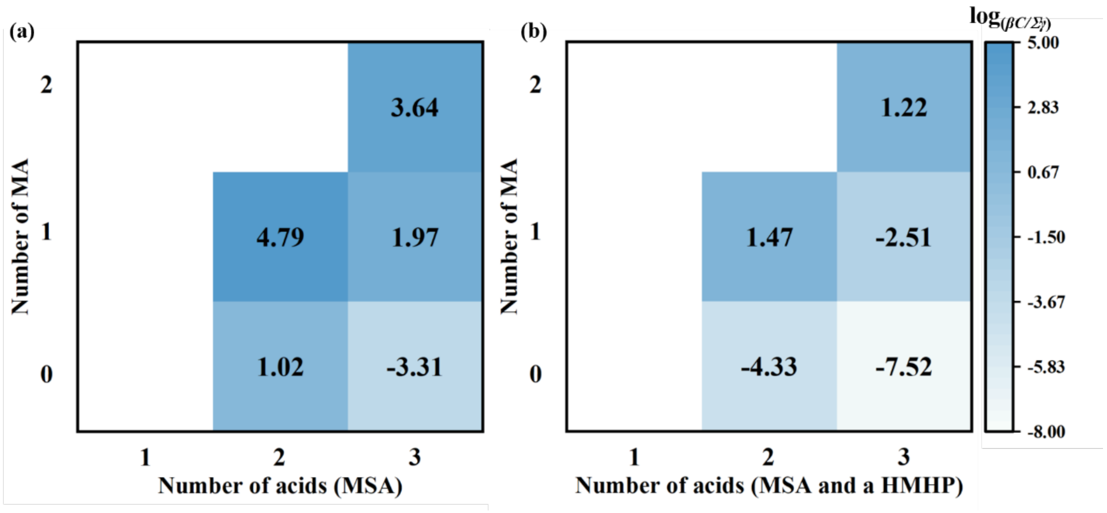

Fig. 4. The log(βC/$\Sigma\gamma$) of $(MSA)_x(MA)_y(HMHP)_z$ ($0 \leqslant y \leqslant x + z \leqslant 3$) clusters at 238.15K. (a) without HMHP monomer, (b) containing a HMHP monomer. The βC/$\Sigma\gamma$ is the ratio of collision frequency between the cluster and monomer molecule at the concentration C to the total evaporation frequency at C = 2.5×10^8 molecules·cm^{-3}.

(b) In Lines 258-272 on Pages 9-10 of the revised manuscript, we have completely rewritten the discussion in section 3.3.2. To evaluate the effect of HMHP on the thermodynamic stability of MSA-MA-clusters, the Gibbs free energy (ΔG) (Table S7) and total evaporation rates ($\Sigma\gamma$) (Table S10) of clusters in the MSA-MA-HMHP system were calculated. The ΔG of HMHP-involved clusters are consistently lower than those of the corresponding pure MSA-MA clusters, indicating that the participation of HMHP enhances cluster thermodynamic stability. Consistent with the ΔG analysis, HMHP-containing clusters also exhibit markedly reduced $\Sigma\gamma$ values. In addition to thermodynamic stability, cluster growth tendencies play a crucial role in atmospheric cluster formation. From a kinetic perspective, cluster formation is governed by the competition between molecular collisions and evaporation processes. When the ratio of the collision frequency between a cluster and a monomer at concentration C to the total evaporation rate, expressed as βC/$\Sigma\gamma$, is higher than 1, the cluster is considered capable of sustained growth. Accordingly, as shown in Fig. 4, the βC/$\Sigma\gamma$ ratios were evaluated under various atmospheric conditions to assess the influence of HMHP on the growth behavior of MSA-MA clusters. Among the clusters examined, $(MSA)_2$, $(MSA)_2\cdot(MA)$, $(MSA)_2\cdot(MA)_2$, $(MSA)_3\cdot(MA)_2$, $(MSA)\cdot(MA)\cdot(HMHP)$ and $(MSA)_2\cdot(MA)_2\cdot(HMHP)$ display sufficient stability against evaporation, enabling further growth through collisions with additional monomers. Overall, these results suggest that HMHP is likely to participate in the nucleation process of MSA-MA clusters by enhancing their thermodynamic stability and increasing their potential for sustained cluster growth.

Comment 8.

Line 268: it is recommended to include the simulation at 298.15 K to cover a more comprehensive temperature range.

Response: Thanks for your valuable comments. As the reviewer's suggestion, we have incorporated simulations at 298.15 K into the study, thereby extending the analysis to a broader and more comprehensive temperature range. The detailed revisions are outlined below.

(a) The Cluster formation pathway of the MSA-MA-HMHP system at 298.15 K is presented in Fig. S3 of the supplement.

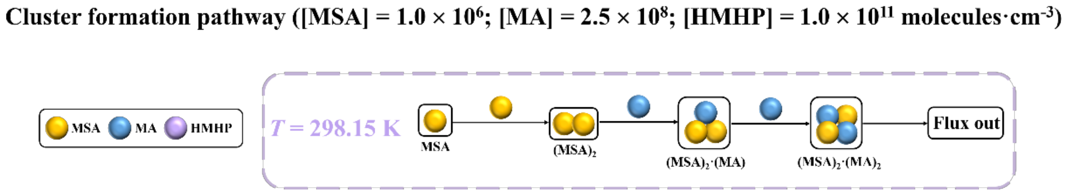

Fig. S3. The Cluster formation pathway of the MSA-MA-HMHP system at 298.15 K.

(b) In Lines 275 on Page 10 of the revised manuscript, the sentence of "To track the detailed nucleation pathways of HMHP involved in the formation of MSA-MA clusters, ACDC simulation were conducted at four different temperatures (238.15 K, 258.15 K, 278.15 K and 298.15 K), with concentrations set as [MSA] = 1.0 ×10^6 molecules·cm^{-3}, [MA] =2.5 × 10^8 molecules·cm^{-3} and [HMHP] = 1.0 ×10^{11} molecules·cm^{-3}." has been added.

(c) In Lines 286-289 on Pages 10-11 of the revised manuscript, the sentence of "However, at 278.15 K, HMHP acts only as a "participant" in the formation of critical clusters. With increasing temperature, the contribution of HMHP to cluster formation diminishes, and at 298.15 K (Fig. S3) cluster formation occurs exclusively through the pure binary MSA-MA pathway." has been added.

Comment 9.

Several minor mistakes should be corrected, for example, Line 156: standardize the use of italics. Please carefully review the entire manuscript

Response: Thanks for your valuable comments. As the reviewer's suggestion, we have systematically reviewed and uniformly corrected the use of italic formatting throughout the entire manuscript. So, in Lines 166 on Page 6 of the revised manuscript, the method level has been changed from "M06-2X/6-311++G(*2df,2pd*)" to "M06-2X/6-311++G(2df,2pd)".

Responses to Referee #2's comments

We are grateful to the reviewers for their valuable and helpful comments on our manuscript "Rapid formation of hydroxymethyl hydroperoxide and its vital role in methanesulfonic acid-methylamine nucleation: impacts of urban industrial and forested areas" (MS No.: **egusphere-2025-4960**). We have revised the manuscript carefully according to reviewers' comments. The point-to-point responses to the Referee #2's comments are summarized below:

General comments:

Major comments: While I am not an expert in quantum calculations or molecular dynamics, this manuscript clearly addresses the enhanced formation of HMHP via MSA-catalyzed hydrolysis of CH_2OO and highlights its importance in new particle formation. The theoretical results presented provide valuable guidance for future research on SA- and MSA-derived nucleation.

However, as shown in Figure 6, the MSA concentrations are around 1×10^4 in all locations, which is near the detection limit of the CIMS, if that is the instrument used. It is unclear how reliable these data are for quantifying MSA's contribution to nucleation or HMHP formation. I suggest that the authors tone down the emphasis on the importance of MSA-HMHP formation in urban industrial regions. Because, as usual, SA-MA or SA-NH_3 are the main nucleation mechanisms in the urban industrial regions.

Specific Comments:

Comment 1.

Lines 53-59: The manuscript should clarify why MSA is important in this study. Its atmospheric abundance varies widely: typically high in the marine atmosphere and free troposphere, but often very low over continental regions. The authors should provide an estimate of the average MSA concentration in continental areas. Compared to H_2O dimers, MSA is much lower in concentration, so the text should explicitly explain why its role in nucleation is significant despite its low abundance.

Response: Thanks for your valuable comments. In fact, MSA, one of the simplest organic organosulfur acids in the atmosphere, is a prominent oxidation product from organosulfur compounds that originate from biological processes, biomass combustion, industrial emissions, and agriculture, which appreciably contribute to atmospheric NPF events in certain conditions (***Chem. Rev.*** 2006, 106, 940-975.; ***Environ. Sci. Technol.***, 2017, 51, 243-252.; ***Environ. Sci. Technol.,*** 2010, 44, 1566-1572). MSA has been measured in atmospheric aerosol particles nearly all geographic regions, ranging from coastal areas to the continental. Notably, in coastal regions characterized by elevated MSA levels, MSA concentrations range from approximately 10% to 250% of gaseous sulfuric acid concentration (***Atmos. Chem. Phys.***, 2022, 22, 6103-6114; ***Atmos. Environ.*** 2022, 269, 118826), whereas in continental regions with lower MSA levels, MSA concentrations are typically ~10%-50% of gaseous sulfuric acid concentrations (***J. Geophys. Res.*** 2002, 107, 7101-7116; ***Atmos. Environ.*** 2020, 222, 117161).

Despite its much lower atmospheric abundance than H_2O, MSA can act as an efficient catalytic species owing to its strong acidity and versatile hydrogen-bonding capability. By forming stable pre-reactive complexes and facilitating multiple proton-transfer pathways, MSA substantially lowers the reaction barriers for CH_2OO hydrolysis.

Based on the above analysis, we emphasized the importance of MSA in the Introduction section. In Lines 54-64 on Pages 2-3 of the revised manuscript, the sentence of "In fact, MSA is a major oxidation product of organosulfur compounds originating from a variety of sources, including biological processes, biomass combustion, industrial emissions, and agricultural activities. As a result, it has been widely detected in atmospheric aerosol particles across diverse geographic regions, spanning from coastal to inland areas (Barnes et al., 2006; Gaston et al., 2010). Notably, in coastal regions characterized by elevated MSA levels, MSA concentrations range from approximately 10% to 250% of gaseous sulfuric acid concentration (Ning et al., 2022; Ning and Zhang, 2022), whereas in continental regions with lower MSA levels, including many inland urban and industrial regions, MSA concentrations are typically on the order of ~10%-50% of gaseous sulfuric acid concentrations (Berresheim et al., 2002; Chen et al., 2020). Furthermore, MSA is characterized by strong acidity and the ability to act as a proton-transfer bridge, suggesting a potentially important role in modulating the hydrolysis of CH_2OO." has been reorganized.

Comment 2.

Lines 79-81: The current sentence about discrepancies between measured and modelled global NPF rates is unclear. It is not accurate to attribute differences solely to MSA-driven nucleation. The authors should clarify that global NPF simulations can be influenced by multiple factors, including missing nucleation mechanisms, NH_3 concentrations, and other environmental parameters. A rephrasing is needed to reflect these more accurately.

Response: Thanks for your valuable comments. As noted by the reviewer, the binary MSA-MA nucleation mechanism underestimates the nucleation rates compared to field observations. Therefore, seeking the involvement of other gaseous species to better understand the MSA-MA-driven NPF. In Lines 85-88 on Page 4 of the revised manuscript, the sentence of "However, the binary MSA-MA nucleation mechanism is insufficient to explain the high NPF rates observed under realistic atmospheric conditions. This implies that other potential gaseous precursors may participate in and further enhance binary MSA-MA nucleation (Lee et al., 2019; Zhang et al., 2022)" has been reorganized.

Comment 3.

Lines 84-85: MSA in urban industrial areas and forested areas are low. And the NPF mechanisms are SA-base plus AP. MSA's importance on NPF in these areas can not convince me.

Response: Thanks for your valuable comments. We sincerely apologize for the insufficiently comprehensive assessment of the impact of HMHP on MSA-MA nucleation in the previous version of the manuscript. The earlier analysis focused primarily on regions with elevated HMHP concentrations, while the concentration distributions of the precursor species MSA and MA were not adequately considered. Indeed, the regions in which HMHP influences the MSA-MA nucleation process should be determined through a comprehensive evaluation of the concentration characteristics of HMHP, MSA and MA. In the revised manuscript, we therefore systematically account for the combined effects of HMHP, MSA and MA concentrations on the formation rate of the HMHP-involved MSA-MA system.

Our results indicate that HMHP's contribution to MSA-MA nucleation is most pronounced under conditions of high HMHP concentrations accompanied by relatively low concentrations of both MSA and MA. A review of the existing literature shows that regions with high HMHP concentrations are mainly associated with urban industrial areas and forested regions, whereas low concentrations of MSA and MA are predominantly observed in urban industrial environments.

Based on these integrated lines of evidence, we predict that the influence of HMHP on the MSA-MA system is most significant in urban industrial regions. The corresponding main revision has been made as follows.

(a) In the revised manuscript, the title of "Rapid formation of hydroxymethyl hydroperoxide and its vital role in methanesulfonic acid-methylamine nucleation: impacts of urban industrial and forested areas" has been changed as "Rapid formation of hydroxymethyl hydroperoxide and its vital role in methanesulfonic acid-methylamine nucleation: impacts of urban industrial areas".

(b) In Lines 91-92 on Page 4 of the revised manuscript, the sentences of "This will limit our knowledge of frequent NPF events, especially in urban industrial areas and forested areas." has been changed as "This will limit our knowledge of frequent NPF events, especially in urban industrial areas."

(c) In Lines 231-232 on Pages 8-9 of the revised manuscript, the sentences of "Finally, the atmospheric implication of HMHP for MSA-MA nucleation were calculated for urban industrial areas and forested areas." has been changed as "Finally, the atmospheric implication of HMHP for MSA-MA nucleation were calculated for urban industrial areas."

(d) In Lines 319-321 on Page 12 of the revised manuscript, the sentences of "These results highlight that HMHP exerts a markedly stronger influence on MSA-MA nucleation at elevated concentrations, particularly in urban industrial and forested regions, where its contribution to NPF can be substantial." has been changed as "These results highlight that HMHP exerts a markedly stronger influence on MSA-MA nucleation at elevated concentrations, particularly in urban industrial regions, where its contribution to NPF can be substantial."

(e) In Lines 351-353 on Page 13 of the revised manuscript, the sentences of "These results predict that HMHP substantially enhances MSA-MA-driven NPF in urban industrial and forested regions, helping to explain previously unaccounted NPF sources and improve nucleation models." has been changed as "These results predict that HMHP substantially enhances MSA-MA-driven NPF in urban industrial regions, helping to explain previously unaccounted NPF sources and improve nucleation models."

(f) In Lines 355-356 on Page 13 of the revised manuscript, the sentences of "It also reveals the potential contribution of other organic peroxides to NPF, offering a plausible explanation for part of the unaccounted particle fluxes in both urban industrial regions." has been changed as "It also reveals the potential contribution of other organic peroxides to NPF, offering a plausible explanation for part of the unaccounted particle fluxes in urban industrial regions."

Comment 4.

Lines 178-180: At this MSA level, the reaction is reported to be more favorable than that with NH_3. How does it compare to the response with H_2O?

Response: Thanks for your valuable comments. Based on the calculated effective rate constants, when the MSA concentration ranges from 10^6 to 10^8 molecules·cm^{-3}, its catalytic effect is substantially stronger than that of NH_3, for which concentrations of 10^7-10^{11} molecules·cm^{-3} are considered. Similarly, at MSA concentrations between 10^5 and 10^8 molecules·cm^{-3}, MSA exhibits significantly higher catalytic activity than SA ([SA] = 10^4-10^7 molecules·cm^{-3}). Taken together, these results indicate that MSA is a more effective catalyst than both NH_3 and SA. Nevertheless, because atmospheric H_2O concentrations are orders of magnitude higher than those of MSA, the overall catalytic efficiency of MSA remains lower than that of H_2O. In Lines 185-193 on Page 7 of the revised manuscript, the sentence of "When the MSA concentration ranges from 10^6 to 10^8 molecules·cm^{-3}, its catalytic effect is substantially stronger than that of NH_3 ([NH_3] = 10^7-10^{11} molecules·cm^{-3}), with k'_{MSA} being approximately 2-6 orders of magnitude over the temperature range of 280.0-320.0 K. Similarly, for MSA concentrations between 10^5 and 10^8 molecules·cm^{-3}, MSA exhibits a significantly higher catalytic activity than SA ([SA] = 10^4-10^7 molecules·cm^{-3}). In this case, k'_{MSA} exceeds k'_{SA} by about 1-3 orders of magnitude. Taken together, these results demonstrate that MSA is a more effective catalyst than both NH_3 and SA under atmospherically relevant conditions. Nevertheless, even under extreme conditions, with MSA at its upper-limit concentration ([MSA] = 10^8 molecules·cm^{-3}) and H_2O at its lower-limit concentration ([H_2O] = 10^{16} molecules·cm^{-3}), k'_{MSA} is approximately five orders of magnitude smaller than $k'_{\mathrm{WM},}$, indicating that the catalytic efficiency of MSA remains lower than that of H_2O." has been reorganized.

Comment 5.

Section 3.3 and 3.4: When assessing the importance of HMHP in MSA-MA nucleation, it is essential to investigate and compare the behavior of HMHP-MSA-MA clusters with that of SA-MA clusters. Such a comparison would help clarify the relative importance of HMHP-MSA-MA nucleation.

Response: Thanks for your valuable comments. In response to the reviewer's suggestion, comparing the formation rates of the MSA-MA-HMHP system with those of the SA-MA and SA-A systems is crucial for assessing the nucleation potential of HMHP. Accordingly, in the revised manuscript, we have included a quantitative comparison of the formation rates (*J*) for the MSA-MA-HMHP, SA-MA and SA-A systems (Fig. S7) and added the corresponding discussion in section 3.4. The corresponding main revision has been made as follows.

(a) In the supplement, the cluster formation rates of the MSA-MA-HMHP systems have been compared to those of the SA-MA (***Atmosphere***, 2024, 15(4), 467) and SA-A (***Atmosphere***, 2024, 15(4), 467) systems, which are widely regarded as key contributors to new particle formation in urban industrial areas (***Environ. Sci. Technol.***, 2021, 55(16), 10994-11005; ***Atmos. Chem. Phys.***, 2021, 55(16), 10994-11005). This corresponding comparison is presented in Fig. S7.

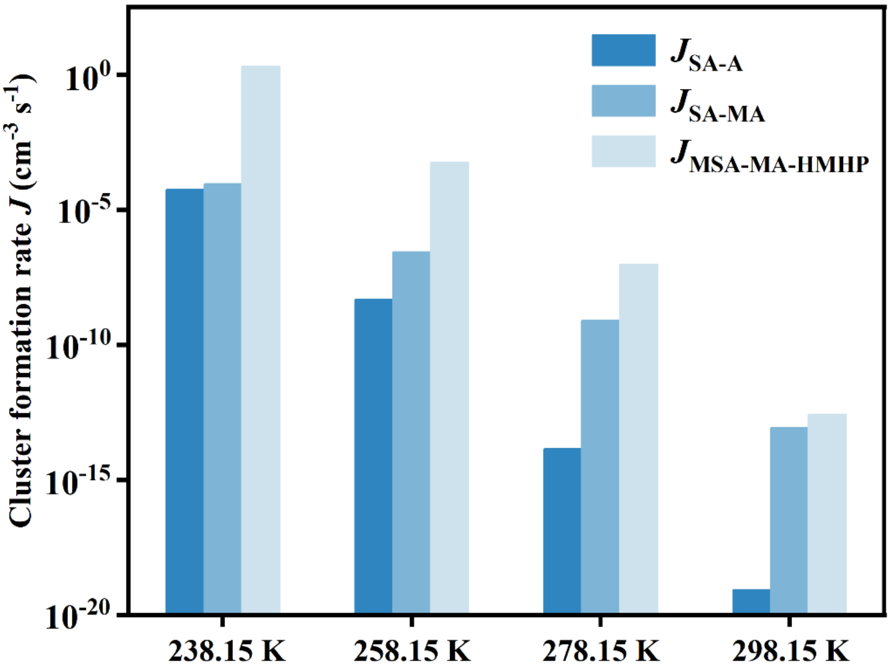

Fig. S7 Comparison of cluster formation rates (*J*) between the MSA-MA-HMHP system ([MSA] = 1.00×10^6 molecules·cm^{-3}, [MA] = 1.00×10^8 molecules·cm^{-3}, [HMHP] = 1.00×10^9 molecules·cm^{-3}), the SA-MA system ([SA] = 1.00×10^6 molecules·cm^{-3}, [MA] = 1.00×10^8 molecules·cm^{-3}) and the SA-A system ([SA] = 1.00×10^6 molecules·cm^{-3}, [A] = 1.00×10^{10} molecules·cm^{-3})

(b) In Lines 322-331 on Page 12 of the revised manuscript, the sentence of "Previous studies have revealed that SA-MA and SA-A nucleation mechanisms are widely regarded as key contributors to new particle formation in urban industrial regions (Yin et al., 2021; Liu et al., 2021).

To underscore the importance of MSA-MA-HMHP nucleation in urban industrial regions, the cluster formation rates (*J*) of the MSA-MA-HMHP system have been compared with those of the SA-MA and SA-A systems (Qiao et al., 2024) (Fig. S7). The results show that, over the temperature range of 238.15 K-298.15 K, the *J* of MSA-MA-HMHP system is 1-5 orders of magnitude higher than that of SA-MA system at equivalent precursor concentrations ([SA] = 1.00×10^6 molecules·cm^{-3} and [MA] = 1.00×10^8 molecules·cm^{-3}). Similarly, under the conditions of [SA] = 1.00×10^6 molecules·cm^{-3} and [A] = 1.00×10^{10} molecules·cm^{-3}, the *J* of MSA-MA-HMHP systems slightly exceeds that of SA-A system by approximately 5-6 orders of magnitude. These comparisons suggest that HMHP plays a key role in enhancing MSA-MA nucleation, particularly in urban industrial environments." has been added.

Comment 6.

Section 3.4: All the locations discussed in this section exhibit extremely low MSA concentrations. It is unclear why a site with higher MSA levels was not selected for analysis. Additionally, it would be important to compare your proposed mechanism with existing pathways such as SA-NH_3, SA-MA, SA-AP, and others. Without such comparisons, the claim regarding the importance of HMHP-MSA-MA nucleation may not be fully justified.

Response: Thanks for your valuable comments. In response to the reviewer's suggestion, we have clarified the rationale for adopting the minimum MSA concentration in Section 3.4 firstly. Then, a comparison of the formation rates between the MSA-MA-HMHP system and the SA-MA and SA-A systems is performed for assessing the nucleation potential of HMHP. The corresponding main revision has been made as follows.

(a) In this study, the concentration of MSA spans a range of 10^4-10^8 molecules·cm^{-3}. As shown in Fig. 5, the contribution of HMHP to MSA-MA nucleation is most pronounced under conditions of low MSA concentrations. Accordingly, in Section 3.4, the MSA concentration is fixed at its lower-limit value ([MSA] = 1.00×10^4 molecules·cm^{-3}).

(b) Previous studies have revealed that the SA-MA and SA-A systems are widely regarded as key contributors to new particle formation in urban industrial regions (***Environ. Sci. Technol.***, 2021, 55(16), 10994-11005; ***Atmos. Chem. Phys.***, 2021, 55(16), 10994-11005). To highlight the importance of MSA-MA-HMHP nucleation in urban industrial regions, the formation rates (*J*) of the MSA-MA-HMHP, SA-MA and SA-A systems are compared (Fig. S7). The detail information is provided in Comment 5. Meanwhile, it is generally acknowledged that new particle formation in urban industrial regions is predominantly governed by SA-base nucleation mechanisms, such as SA-MA and SA-A, whereas the contribution of SA-AP nucleation is comparatively minor.

Comment 7.

Lines 330-332: What is the main nucleation mechanism in Niwot Ridge and the southeastern United States? Is MSA-MA-driven NPF the main mechanism there?

Response: Thanks for your valuable comments. As the reviewer's suggestion, in the revised manuscript, the dominant formation pathways for Niwot Ridge (Fig. S5) and the southeastern United States (Fig. S6) have been added. Correspondingly, the associated discussion has been incorporated into Section 3.4. The corresponding main revision has been made as follows.

(a) In the supplement, the cluster formation pathways in Niwot Ridge (Fig. S5) and the southeastern United States (Fig. S6) are presented.

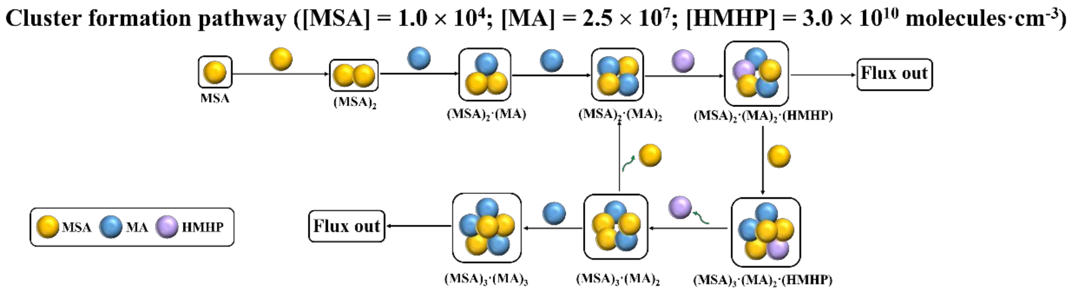

Fig. S5 The cluster formation pathway of the MSA-MA-HMHP system at [MSA] = 1.0 × 10^4 molecules·cm^{-3}, [MA] = 2.5 × 10^7 molecules·cm^{-3} and [HMHP] = 3.0 × 10^{10} molecules·cm^{-3}.

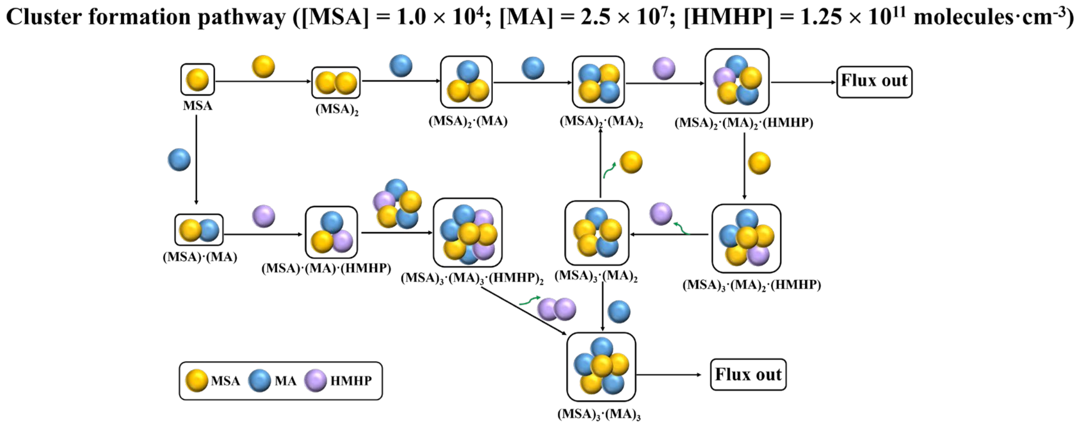

Fig. S6 The cluster formation pathway of the MSA-MA-HMHP system at [MSA] = 1.0 × 10^4

molecules·cm^{-3}, [MA] = 2.5 × 10^7 molecules·cm^{-3} and [HMHP] = 1.25 × 10^{11} molecules·cm^{-3}.

(b) In Lines 315-319 on Page 12 of the revised manuscript, the sentence of "In contrast, in environments characterized by high HMHP concentrations, such as the southeastern United States (1.25 × 10^{11} molecules·cm^{-3}) and Niwot Ridge (3.00 × 10^{10} molecules·cm^{-3}), HMHP-involving nucleation pathways become dominant. Under these conditions, HMHP acts both as a "catalyst", facilitating the formation of MSA-MA clusters, and as an "participant" in the assembly of critical clusters (Figs. S5 and S6). These two roles contribute up to 59% and 42%, respectively, to the overall nucleation process." has been reorganized.

Comment 8.

Figure 6: Please clarify the sources of the vapor concentrations used in this figure. Where were these values obtained?

Response: Thanks for your valuable comments. We apologize for not clearly explaining the settings of the MSA, MA and HMHP concentrations in Fig. 6. A detailed explanation is provided below.

(a) As shown Fig. 5, lower concentrations of MSA and MA tend to enhance the role of HMHP in MSA-MA nucleation. Accordingly, the concentrations of MSA and MA in Fig. 6 are set to low values ([MSA] = 1.00 × 10^4 molecules·cm^{-3} and [MA] = 2.50 × 10^7 molecules·cm^{-3}).

(b) Atmospheric HMHP concentrations exhibit substantial variability across different environments worldwide. Accordingly, to further evaluate the implication of HMHP in the MSA-MA nucleation. Fig. 6 presents an analysis of the branch ratios of the major flux-out pathways under varying HMHP concentrations (2.50 × 10^9 molecules·cm^{-3}-1.25 × 10^{11} molecules·cm^{-3}).

Overall, in Fig.6, the concentrations of MSA and MA are fixed at [MSA] = 1.00 × 10^4 molecules·cm^{-3} and [MA] = 2.50 × 10^7 molecules·cm^{-3}, respectively. Atmospheric HMHP concentrations are then prescribed according to observations from different regions: values range from 2.50 × 10^9 to 6.25 × 10^9 molecules·cm^{-3} in Central Portugal, Pabstthum, and Beijing; increase to 1.15 × 10^{10}-3.00 × 10^{10} molecules·cm^{-3} in Guang Zhou and Niwot Ridge and reach 1.25 × 10^{11} molecules·cm^{-3} in the southeastern United States.